EBioMedicine 24 (2017) 247–256

Contents lists available at ScienceDirect

EBioMedicine

journal homepage: www.ebiomedicine.com

Research Paper

CXCL14 Acts as a Specific Carrier of CpG DNA into Dendritic Cells and Activates Toll-like Receptor 9-mediated Adaptive Immunity

Kosuke Tanegashima [a,*], Rena Takahashi [a,b], Hideko Nuriya [c], Rina Iwase [a,d], Naoto Naruse [e], Kohei Tsuji [e], Akira Shigenaga [e], Akira Otaka [e], Takahiko Hara [a,b,*,1]

[a] Stem Cell Project, Tokyo Metropolitan Institute of Medical Science, 2-1-6 Kamikitazawa, Setagaya-ku, Tokyo 156-8506, Japan
[b] Graduate School of Medical and Dental Sciences, Tokyo Medical and Dental University, 1-5-45 Yushima, Bunkyo-ku, Tokyo 113-8510, Japan
[c] Core Technology and Research Center, Tokyo Metropolitan Institute of Medical Science, 2-1-6 Kamikitazawa, Setagaya-ku, Tokyo 156-8506, Japan
[d] Department of Biological Sciences, Faculty of Science and Engineering, Chuo University, 1-13-27 Kasuga, Bunkyo-ku, Tokyo 112-8551, Japan
[e] Institute of Biomedical Sciences and Graduate School of Pharmaceutical Sciences, Tokushima University, Shomachi, Tokushima 770-8505, Japan

ARTICLE INFO

Article history:
Received 2 June 2017
Received in revised form 3 September 2017
Accepted 12 September 2017
Available online 14 September 2017

Keywords:
CXCL14
TLR9
CpG DNA
Dendritic cells

ABSTRACT

CXCL14 is a primordial chemokine that plays multiple roles in tumor suppression, autoimmune arthritis, and obesity-associated insulin resistance. However, the underlying molecular mechanisms are unclear. Here, we show that CXCL14 transports various types of CpG oligodeoxynucleotide (ODN) into the endosomes and lysosomes of bone marrow-derived dendritic cells (DCs), thereby activating Toll-like receptor 9 (TLR9). A combination of CpG ODN (ODN2395) plus CXCL14 induced robust production of IL-12 p40 by wild-type, but not Tlr9-knockout, DCs. Consistent with this, ODN2395-mediated activation of DCs was significantly attenuated in Cxcl14-knockout mice. CXCL14 bound CpG ODN with high affinity at pH 7.5, but not at pH 6.0, thereby enabling efficient delivery of CpG ODN to TLR9 in the endosome/lysosome. Furthermore, the CXCL14-CpG ODN complex specifically bound to high affinity CXCL14 receptors on DCs. Thus, CXCL14 serves as a specific carrier of CpG DNA to sensitize TLR9-mediated immunosurveillance.

1. Introduction

Innate immune responses are initiated by microbe-derived products known as pathogen-associated molecular patterns (PAMPs) (Blasius and Beutler, 2010; Kawai and Akira, 2010). PAMPs activate pattern recognition receptors (PPRs) expressed on or in dendritic cells (DCs), thereby triggering inflammatory reactions, interferon responses, and DC maturation; these are followed by activation of the adaptive immune response that completely eliminates the pathogen (Blasius and Beutler, 2010; Kawai and Akira, 2010). Among the known PPRs, Toll-like receptor 9 (TLR9) recognizes unmethylated cytosine-phosphate guanine (CpG)-containing DNA (CpG DNA) present in bacterial DNAs; this type of DNA is less abundant in mammalian genomic DNA (Hemmi et al., 2000; Ishii and Akira, 2006). Thus, unmethylated CpG DNA acts as a sensor for TLR9-mediated immunosurveillance (Krug et al., 2004a,b; Lund et al., 2003; Tabeta et al., 2004).

Basic and clinical research studies have used synthetic CpG oligodeoxynucleotide (CpG ODN) as a ligand for TLR9 (Krieg, 2006; Ishii and Akira, 2006). Agonistic CpG ODN molecules fall into four main categories, A, B, C, and P, based on their structure and function. A-class CpG ODNs possess poly-G and palindromic sequences that have strong interferon-α-inducing activity in plasmacytoid DCs (pDCs). B-class CpG ODNs do not contain palindromic sequences and predominantly act on B cells. C-class CpG ODNs have the properties of both A-class and B-class molecules, and include palindromic sequences at the 3′-end. P-class CpG ODNs have two copies of a palindromic sequence and are more potent than C-class molecules with respect to induction of cytokine production.

Since TLR9 is localized within the endosomes and lysosomes of DCs, CpG DNA must be internalized prior to binding. CpG ODNs bind to DEC205 and mannose receptors to trigger TLR9-dependent responses (Lahoud et al., 2012; Caminschi et al., 2013; Moseman et al., 2013). Granulin, HMGB1, LL-37, and β-defensin also facilitate incorporation of CpG ODNs (Park et al., 2011; Ivanov et al., 2007; Hurtado and Peh, 2010; Tewary et al., 2013). Some of these secreted factors directly bind to CpG ODNs (Park et al., 2011; Ivanov et al., 2007; Tewary et al., 2013); however, it is not clear how CpG ODNs are transported into DCs to activate the TLR9 signaling.

CXCL14 is a non-ELR (glutamic acid-leucine-arginine) chemokine with multiple immunological functions (Lu et al., 2016; Hara and Tanegashima, 2012). At very high concentrations, CXCL14 acts as a

* Corresponding authors.
E-mail addresses: tanegashima-ks@igakuken.or.jp (K. Tanegashima), hara-tk@igakuken.or.jp (T. Hara).
[1] Lead contact.

http://dx.doi.org/10.1016/j.ebiom.2017.09.012

chemoattractant for DCs, activated macrophages, and NK cells (Hara and Tanegashima, 2012). Consistent with this, CXCL14 promotes NK cell-mediated suppression of transplanted melanoma cell metastasis in a CXCL14 transgenic mouse line (Hata et al., 2015). CXCL14 transgenic mice with collagen-induced arthritis show augmented Th1 responses (Chen et al., 2010). Conversely, Cxcl14-knockout (KO) mice show weaker inflammatory responses when they become obese (Nara et al., 2007). Although these results clearly indicate that CXCL14 is involved in Th1 immune responses, the underlying molecular mechanisms require clarification.

Since CXCL14 is abundantly present in mucosal tissues (the Human Protein Atlas: http://www.proteinatlas.org/ENSG00000145824-CXCL14/tissue) and displays anti-microbial activity, we speculated that CXCL14 might be involved in innate immunity. Here, we demonstrate that CXCL14 specifically binds CpG DNAs, delivers them to the endosomal/lysosomal compartments in DCs via receptor internalization, and efficiently activates TLR9-mediated cytokine production and DC maturation.

2. Materials and Methods

2.1. Mice and Cell Preparation

C57BL/6N mice were obtained from Nihon SLC (Hamamatsu, Japan). As previously described (Tanegashima et al., 2010), *Cxcl14*$^{-/-}$ male and Cxcl14$^{+/-}$ female mice with a C57BL/6 N background were crossed to produce Cxcl14$^{+/-}$ and *Cxcl14*$^{-/-}$ mice. LysM-Cre knock-in mice (Clausen et al., 1999) were obtained from RIKEN (RBRC02302), and CD11c-Cre (stock number 007567) and Cxcr4$^{F/F}$ (stock number 008767) mice were obtained from the Jackson Laboratory (Bar Harbor, ME). Tlr9-KO mice (Hemmi et al., 2000) were obtained from Oriental Bioservice, Inc. (Kyoto, Japan).

BMDCs were prepared from 6-week-old C57BL/6N, Tlr9-KO, and Cxcr4-CKO mice by culturing bone marrow cells in RPMI-1640 medium (Nacalai Tesque, Kyoto, Japan) containing 10% fetal bovine serum (Thermo Fisher Scientific, Waltham, MA), mouse granulocyte-macrophage colony stimulating factor (10 ng/ml; Peprotech, Rocky Hill, NJ), and mouse IL-4 (10 ng/ml; Peprotech) for 10 days. Splenocytes were prepared from spleen removed from 6 to 8 week-old C57BL/6N mice. Red blood cells were lysed in RBC lysis buffer (140 mM NH_4Cl, 17 mM Tris-HCl, pH 7.6). All mice were housed in a pathogen-free animal facility under a 12 h light/dark cycle. All experimental procedures were pre-approved by the ethical committee of Tokyo Metropolitan Institute of Medical Science.

2.2. Reagents

Endotoxin-free ODN2395 was purchased from InvivoGen (San Diego, CA). ODN2395mut (phosphorothioester modified sequence), 5′Cy3-ODN2395, 5′Cy3-ODN2395(p), 5′Cy3-ODN2395mut(p), ODN1826, ODN1826(p), 5′Cy3-ODN1826, 5′Cy3-ODN1826(p), ODN1585(p), 5′Cy3-ODN1585(p), ODN-D-SL03, 5′Cy3-ODN-D-SL03, ODN21798, 5′Cy3-ODN21798, ODN1668, ODN1668(p), 5′Cy3-ODN1668, 5′Cy3-ODN1668(p), and 5′Cy3-D35 were synthesized by Eurofins Genomics (Tokyo, Japan). D35 was purchased from Gene design (Osaka, Japan). CXCL14, CXCL14-K-biotin (referred to as CXCL14-bio in this study), and CXCL14-Alexa488 were chemically synthesized (Tsuji et al., 2015) based on the human CXCL14 sequence (Supplementary methods and Fig. S1). Synthetic CXCL14 was as active as recombinant CXCL14 in terms of the inhibition of CXCL12-mediated cell migration. The endotoxin level of the synthetic CXCL14 preparation was <0.1 EU/mg, as measured by a LAL Quantitation Kit (Thermo Fisher Scientific). LPS, Poly-U, and Poly-IC were purchased from Sigma-Aldrich (St. Louis, MO).

2.3. Antibodies

The following antibodies/conjugates were purchased: Allophycocyanin (APC)-conjugated anti-CD3ε (TONBO, Cat# 20–0032, RRID:AB_2621538, Burlingame, CA), fluorescein isothiocyanate (FITC)-conjugated anti-CD8α (BioLegend, Cat# 100706, RRID:AB_312745, San Diego, CA), APC-rat anti-CD45R/B220 (BioLegend, Cat# 103212, RRID:AB_312997), Brilliant Violet (BV) 421-conjugated anti-CD11c (BioLegend, Cat# 117329 RRID:AB_10897814), AlexaFluor488-anti-CD11b (BioLegend), FITC-anti-CD19 (BioLegend, Cat# 152404 RRID:AB_2629813), FITC-anti-CD3ε (BioLegend, Cat# 100203 RRID:AB_312660), APC-anti-CD184 (CXCR4; BioLegend, Cat# 146508 RRID:AB_2562785), phycoerythrin (PE)-conjugated anti-MHC class II (BD Biosciences, San Jose, CA), PE-anti-CD86 (BioLegend, Cat# 105106 RRID:AB_313159), mouse anti-EEA1 (eBioscience, San Diego, CA), Alexa488-labeled goat anti-mouse IgG, and FITC-anti-LAMP1 (BioLegend, Cat# 121606 RRID:AB_572007).

2.4. FACS Analysis

BMDCs were stained with a BV421-labeled anti-CD11c antibody to confirm DC differentiation. Splenic cells were stained to identify CD8$^+$ cDCs (BV421-CD11c$^+$/FITC-CD8$^+$/APC-CD3ε$^-$/APC-CD45R/B220$^-$), CD11b$^+$ cDCs (BV421-CD11c$^+$/Alexa488-CD11b$^+$/APC-CD3ε$^-$/APC-CD45R/B220$^-$), and pDCs (BV421-CD11c$^+$/FITC-CD19$^-$/FITC-CD3ε$^-$/APC-CD45R/B220$^+$). Cells were analyzed using a LSR Fortessa X-20 cytometer (BD Biosciences).

2.5. FACS and Microscopic Analyses of Incorporated CpG ODNs

BMDCs were plated onto 24 well plates (10^5 cells/well; Corning, Corning, NY) and incubated for 1 h at 37 °C with Cy3-ODNs in the presence or absence of CXCL14 or CXCL12 in RPMI-1640 medium containing 20 mM Hepes-NaOH, pH 7.5, and 0.1% BSA (Sigma, fatty acid free). Cells were then trypsinized, stained with BV421-labeled anti-CD11c, and analyzed by FACS.

For confocal microscopy analysis, BMDCs were plated onto 35 mm glass plates (IWAKI, Tokyo, Japan) and incubated for 1 h at 37 °C with CXCL14-Alexa488, Cy3-ODN2395, or Cy3-ODN2395 + CXCL14 in RPMI-1640/20 mM Hepes-NaOH pH 7.5/0.1% BSA. Cells were then fixed with 4% paraformaldehyde/PBS for 1 h, permeabilized in 0.04% Saponin/PBS (Wako, Osaka, Japan), and stained with anti-EEA1 or anti-LAMP1 antibodies. Fluorescent images were analyzed using a Leica TCS SP8 confocal microscope (Leica Microsystems, Wetzlar, Germany).

2.6. Enzyme-Linked Immunoassay (ELISA)

BMDCs were plated onto 24-well plates (10^5 cells/well) (Corning) and incubated in RPMI-1640/20 mM Hepes-NaOH pH 7.5/0.1% BSA for 6 h at 37 °C with CpG ODNs in the presence or absence of CXCL14 or CXCL12. Culture supernatants were then tested using ELISA MAX™ Kits (BioLegend).

2.7. In Vitro Binding Assay

CXCL14-bio (10 pmol) was coupled to streptavidin-agarose (Sigma-Aldrich) and incubated with Cy3-ODN [100 nM in 100 μl of binding buffer (50 mM Hepes pH 7.5, 150 mM NaCl, 1 mM $CaCl_2$, 1 mM $MgCl_2$, 1% BSA)] for 1 h at 4 °C. Precipitates were then washed and eluted in SDS sample buffer at 70 °C for 10 min. Cy3-ODN was separated by TBE-Urea-SDS polyacrylamide gel electrophoresis, and Cy3 fluorescence was measured in a LAS-3000 (Fuji Film, Tokyo, Japan). CXCL14-bio was blotted onto a PVDF membrane and incubated with peroxidase-conjugated streptavidin (GE Healthcare, Pittsburgh, PA). Chemiluminescence detection was performed using the ECL Plus detection reagent (GE Healthcare), and signals were measured in a LAS-3000.

2.8. Scatchard Plot Analysis

CXCL14-bio [10 pmol for ODN or 100 pmol for ODN(p)] was incubated for 1 h at 4 °C with streptavidin-agarose and Cy3-ODN in 100 μl of 50 mM Hepes pH 7.5/150 mM NaCl/1 mM $CaCl_2$/1 mM $MgCl_2$/1% BSA. The supernatant was collected and used as free Cy3-ODN. Bound Cy3-ODN was eluted by heating at 56 °C for 1 h in 100 μl of elution buffer [Tris-HCl pH 7.5, 200 mM NaCl, 5 mM EDTA, 1% SDS, proteinase K (0.02 mg/ml)]. Cy3 fluorescence was then measured in a Varioskan Flash apparatus (Thermo Fisher Scientific). The bound/free ratio was then plotted against bound Cy3-ODN (nM). The slope of the liner regression line was determined, and K_d was calculated as follows: −1 divided by the slope of the liner regression line.

2.9. Cell Surface Binding Assay

293 T cells were transfected with a pCS2 + mouse *Dec205* expression vector using polyethyleneimine HCl MAX (Polysciences, Warrington, PA). Twenty-four hours after transfection, BMDCs, 293 T cells, and *Dec205*-transfected 293 T cells were trypsinized, resuspended in 50 mM Hepes pH 7.5/150 mM NaCl/1 mM $CaCl_2$/1 mM $MgCl_2$/1% BSA, and incubated with Cy3-ODN2395 in the presence or absence of CXCL14 for 1 h at 4 °C. Cells were then subjected to FACS using a LSR Fortessa X-20 cytometer. Data were analyzed using GraphPad Prism software (GraphPad Software, La Jolla, CA).

2.10. In Vivo Administration of CpG ODNs

Serum was collected from mice 3 days prior to injection and used as a steady state sample. Three individual mice received an intravenous injection of ODN2395 (20 nmol), and serum and spleen samples were obtained 24 h later.

2.11. Statistical Analyses

Each of in vitro experiments was done more than twice with triplicate samples. All statistical analyses were performed using Microsoft Excel and an unpaired Student's *t*-test. Bar graphs present data as the mean ± standard error. The mean fluorescent intensity and the percentage of $Cy3^{high}$ cells were calculated by FlowJo software (Tomy Digital, Tokyo, Japan). A P-value < 0.05 was considered significant.

3. Results

3.1. Hypothesis of CXCL14 and DNA Interaction

Since an isoelectric point of CXCL14 is 10.3, we suspected that CXCL14 might bind to DNA. We first noticed that CXCL14 and plasmid DNA produced insoluble precipitates when they were mixed together (Fig. S2a). More importantly, CXCL14 promoted incorporation of GFP expression vector into HeLa cells (Fig. S2b). Since CXCL14 is known to be involved in the Th1-associated inflammation, we tested the possibility that CXCL14 functionally interacts with CpG ODNs, strong inducers of Th1 response.

3.2. CXCL14 Promotes Internalization of CpG DNA by DCs

First of all, we performed FACS-based internalization assays of Cy3-labeled CpG ODNs. Mouse bone marrow-derived DCs (BMDCs) were incubated with Cy3-labeled ODN2395(p), a representative C-class CpG ODN (Roda et al., 2005) [(p) denotes ODN containing natural phosphodiester bonds], in the presence or absence of CXCL14. BMDCs incorporated very little Cy3-ODN2395(p) alone; however, internalization was enhanced markedly by addition of 300 nM CXCL14 [Fig. 1a (upper panels) and 1b]. CXCL14 also increased uptake of Cy3-ODN2395 (phosphorothioated form) by BMDCs [Fig. 1a (lower panels) and 1b]; ODN2395 has been used widely in vaccine adjuvant studies in the past. Internalization was weak when we tested CXCL12, excluding the possibility that DNA bound to CXC-type chemokines non-specifically. Moreover, we also observed CXCL14-assisted incorporation of Cy3-ODN2395(p) and Cy3-ODN2395 by $CD11c^+CD8^+$ conventional DCs (cDCs) (Fig. 1c and d), $CD11c^+CD11b^+$ cDCs, and plasmacytoid DCs (pDCs) isolated from mouse spleens (Fig. S3).

3.3. CXCL14 Interacts With Various Types of CpG ODN

Next, we examined the effect of CpG ODN sequence/structure on its transportation by CXCL14. The sequences of the CpG ODNs examined are shown in the Table 1. First, in the presence of CXCL14, BMDCs incorporated Cy3-ODN2395mut(p) (in which CpG dinucleotides are replaced by GpC dinucleotides) as efficiently as Cy3-ODN2395(p) (Fig. 1e and f), suggesting that the CpG sequence has no effect on CXCL14-mediated intracellular transport. Next, we found that CXCL14 did not support internalization of Cy3-ODN1826(p), a representative B-class CpG ODN lacking a palindromic structure (Fig. 1e and f). However, uptake of Cy3-ODN1826 (phosphorothioated form) was enhanced (Fig. S4). ODN1668 is another B-class CpG ODN, which is specific to mouse (Heit et al., 2004). As was observed in ODN1826, CXCL14 supported internalization of phosphorothioated Cy3-ODN1668, but not phosphodiestered Cy3-ODN1668(p) (Fig. S5). Finally, we found that Cy3-ODN1585(p), a representative A-class CpG ODN, was incorporated by BMDCs, and that this was not enhanced by CXCL14 (Fig. 1e and f). We found it interesting that CXCL14 also promoted transport of a methylated form of ODN2395, albeit at a slightly reduced rate (Fig. 1g and h). CXCL14 also increased intracellular transport of ODN-D-SL03 (C-class), ODN21798 (P-class), and D35 (A-class), all of which are highly potent CpG ODNs (Yang et al., 2013; Samulowitz et al., 2010; Gursel et al., 2002) (Fig. S4). Taken together, these data suggest that CXCL14 recognizes a sequence/structure common to C-class, phosphorothioated form of B-class, P-class, and a part of A-class CpG ODNs.

3.4. Co-localization of CpG ODN and CXCL14 Within the Endosome/Lysosome

We next used confocal microscopy to examine whether CpG ODN is internalized together with CXCL14. When BMDCs were incubated with Cy3-ODN2395 plus CXCL14 C-terminally conjugated to Alexa488 (CXCL14-Alexa488), almost all Cy3-positive foci in the peri-nuclear region were positive for CXCL14-Alexa488, suggesting co-localization (Fig. 2a). Although CXCL14-Alexa488 was also incorporated by BMDCs in the absence of Cy3-ODN2395, the fluorescent signals were weaker (Fig. 2a). Moreover, very weak Cy3 signals were detected when BMDCs were incubated with Cy3-ODN2395 alone (Fig. 2b and c).

Next, we examined the subcellular localization of internalized CpG ODN/CXCL14. Cy3-ODN2395/CXCL14-loaded BMDCs were stained with an antibody specific for EEA1 (an endosome marker) or LAMP1 (a lysosome marker). The Cy3-positive foci merged with the EEA1 and LAMP1 signals (Fig. 2b and c). These results indicate that CXCL14 acts as a carrier molecule that escorts C-class CpG ODNs to the endosomal/lysosomal compartments.

3.5. CXCL14 Supports CpG ODN-mediated Cytokine Production and DC Maturation

Since CpG ODN is an agonistic ligand for TLR9, we investigated the cytokine-inducing capacity of CXCL14 using BMDCs as a readout for the TLR9 signal. A combination of ODN2395 and CXCL14 induced much greater production of interleukin (IL)-12 p40, IL-6, and tumor necrosis factor (TNF)-α than either molecule alone (Fig. 3a–c). A negative control, ODN2395mut (which lacks TLR9 binding capacity), had no effect on cytokine production in the presence of CXCL14. Importantly, CXCL14 had no synergistic effect on production of IL-12 p40 and IL-6 in the presence of polyinosinic-polycytidylic acid (poly-IC) or

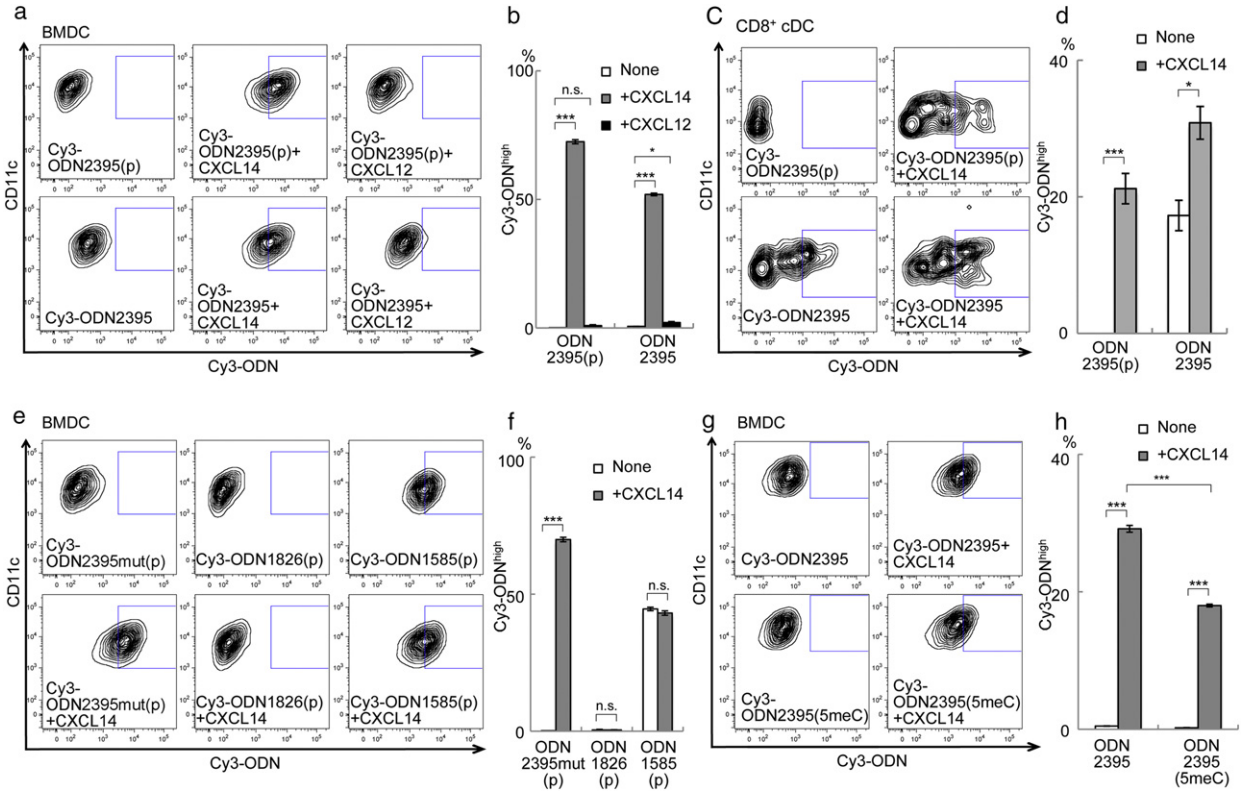

Fig. 1. CXCL14 induces transport of CpG ODN into bone marrow-derived dendritic cells (BMDCs). (a) FACS analysis of $CD11c^+$ BMDCs incubated with 100 nM Cy3-ODN2395(p) or 30 nM Cy3-ODN2395 in the presence or absence of 300 nM CXCL14 or CXCL12 at 37 °C for 1 h. (b) Percentage of Cy3-ODN^{high} cells in (a). (c) FACS analysis of $CD11c^+/CD8^+$ splenic DCs ($CD8^+$cDC) incubated with 100 nM Cy3-ODN2395(p) or 30 nM Cy3-ODN2395 in the presence or absence of 300 nM CXCL14. (d) Percentage of Cy3-ODN^{high} cells in (c). (e) FACS analysis of $CD11c^+$ BMDCs incubated with 100 nM Cy3-ODN2395mut(p), 100 nM Cy3-ODN1826(p), or 100 nM Cy3-ODN1585(p) in the presence or absence of 300 nM CXCL14. (f) Percentage of Cy3-ODN^{high} cells in (E). (g) FACS analysis of $CD11c^+$ BMDCs incubated with 30 nM Cy3-ODN2395 or 30 nM Cy3-ODN2395(5meC) in the presence or absence of 300 nM CXCL14. (h) Percentage of Cy3-ODN^{high} cells in (g). In a, c, e, and g, the Cy3-ODN^{high} fractions are boxed. In b, d, f, and h, each value represents the mean ± standard error (SE) ($n = 3$; $^*P < 0.05$, $^{**}P < 0.01$, $^{***}P < 0.001$; n.s., not significant).

polyuridylic acid (Poly-U) (Fig. 3a–c). CXCL14 alone inhibited Poly-U-induced TNF-α production (Fig. 3c). These data indicate that CXCL14 is not involved in activating TLR3 and TLR7. Consistent with the FACS data (Fig. 1a), we found that CXCL12 did not increase the ODN2395-mediated production of IL-12 p40, IL-6, and TNF-α by BMDCs (Fig. 3d–f). Similar to ODN2395, CXCL14 increased production of IL-12 p40 and IL-6 by BMDCs stimulated with ODN-D-SL03, ODN21798, ODN1826, and ODN1668 (Fig. S6a, S6b, S5c, and S5d). D35 had no effect on the production of IL-12 p40 and IL-6 by BMDCs (Fig. S6a and S6b). It is noteworthy that D35-mediated IFN-α production by pDCs was inhibited by CXCL14; the reason for this is unclear (Fig. S6c).

To verify that the synergistic activity of ODN2395 plus CXCL14 is dependent on TLR9, we next examined cytokine production by BMDCs isolated from Tlr9-KO mice. BMDCs from these mice did not produce IL-12 p40, IL-6, or TNF-α after stimulation with ODN2395 plus CXCL14 (Fig. 3g–i). For these experiments, lipopolysaccharide (LPS) was used as a positive control.

Lastly, we compared cell surface expression of CD86, a representative T cell costimulatory molecule, by BMDCs stimulated with or without ODN2395 plus CXCL14. ODN2395 induced low level expression of CD86, but this increased markedly in the presence of CXCL14 (Fig. 3j and k).

Table 1
Sequences and structures of CpG ODNs.

ODN	K_d (nM)	Nucleotide sequence (5′ to 3′)	Palindrome
ODN2395	9.8	t*c*g*t*c*g*t*t*t*t*c*g*g*c*g*c*g*c*g*c*c*g	+
ODN2395(5meC)	100	t*mc*g*t*mc*g*t*t*t*t*mc*g*g*mc*g*mc*g*mc*g*mc*mc*g	+
ODN2395(p)	58.1	tcgtcgttttcggcgcgcgccg	+
ODN2395mut(p)	59.2	tgctgcttttgggggggcccccc	+
ODN1826(p)	N.D.	tccatgacgttcctgacgtt	−
ODN1826(s)	28	t*c*c*a*t*g*a*c*g*t*t*c*c*t*g*a*c*g*t*t	−
ODN1668(p)	1250	tccatgacgttcctgatgct	−
ODN1668(s)	83	t*c*c*a*t*g*a*c*g*t*t*c*c*t*g*a*t*g*c*t	−
ODN1585(p)	107	ggggtcaacgttgaggggggg	+
ODN-D-SL03	125	t*c*g*c*g*a*a*c*g*t*t*c*g*c*c*g*c*g*t*t*c*g*a*a*c*g*c*g*g	+
ODN21798	80	t*cg*t*cg*t*cg*a*t*cg*g*c*g*cg*c*g*c*c*g	+
D35	77.5	g*gtgcatcgatgcagggg*g*g	+

N.D., not detectable.
*Phosphorothioate bond.
mc, 5′methyl-cytosine.

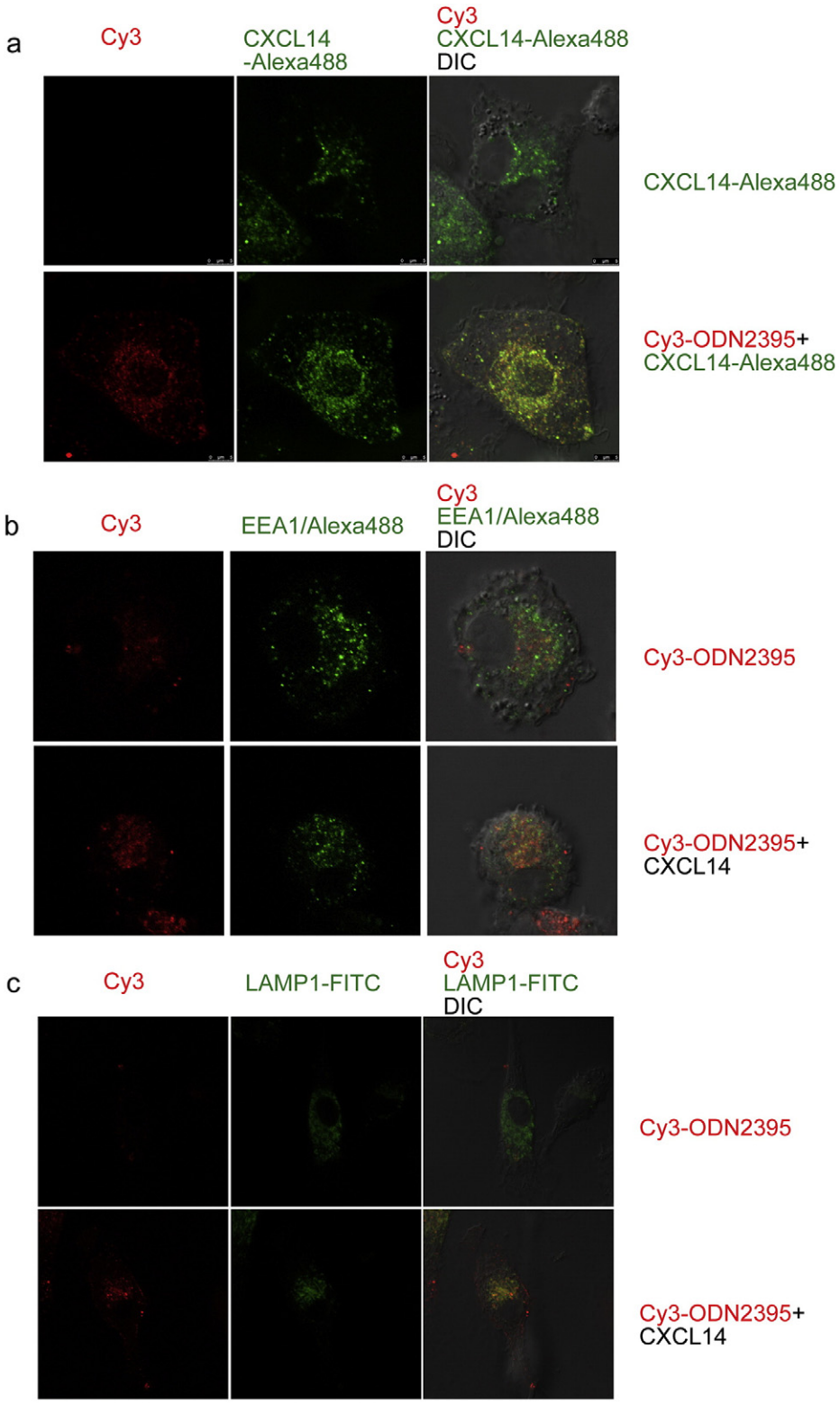

Fig. 2. Intracellular co-localization of CpG ODN and CXCL14. (a) Fluorescence images of BMDCs incubated with 1 μM Alexa488-conjugated CXCL14 in the presence or absence of 30 nM Cy3-ODN2395 at 37 °C for 1 h. (b, c) Fluorescence images of BMDCs incubated with 30 nM Cy3-ODN2395 in the presence or absence of 300 nM CXCL14 at 37 °C for 1 h. Cells were fixed and stained with an anti-EEA1 antibody, followed by an Alexa488-conjugated secondary antibody (b) or a FITC-conjugated anti-LAMP1 antibody (c).

3.6. CXCL14 Binds to CpG ODN With High Affinity

The co-localization and synergistic activities of CpG ODN and CXCL14 led us to investigate whether they directly bind to each other. We first synthesized biotinylated CXCL14 (CXCL14-bio), which retains CpG ODN escort activity (Fig. S7). When Cy3-ODN2395 and CXCL14-bio were incubated in a tube, they formed a stable complex that was precipitated by streptavidin-agarose beads (Fig. 4a). The Cy3-ODN2395/CXCL14-bio was out-competed by excess unlabeled ODN2395, thereby confirming a specific interaction (Fig. 4a). Furthermore, CXCL14

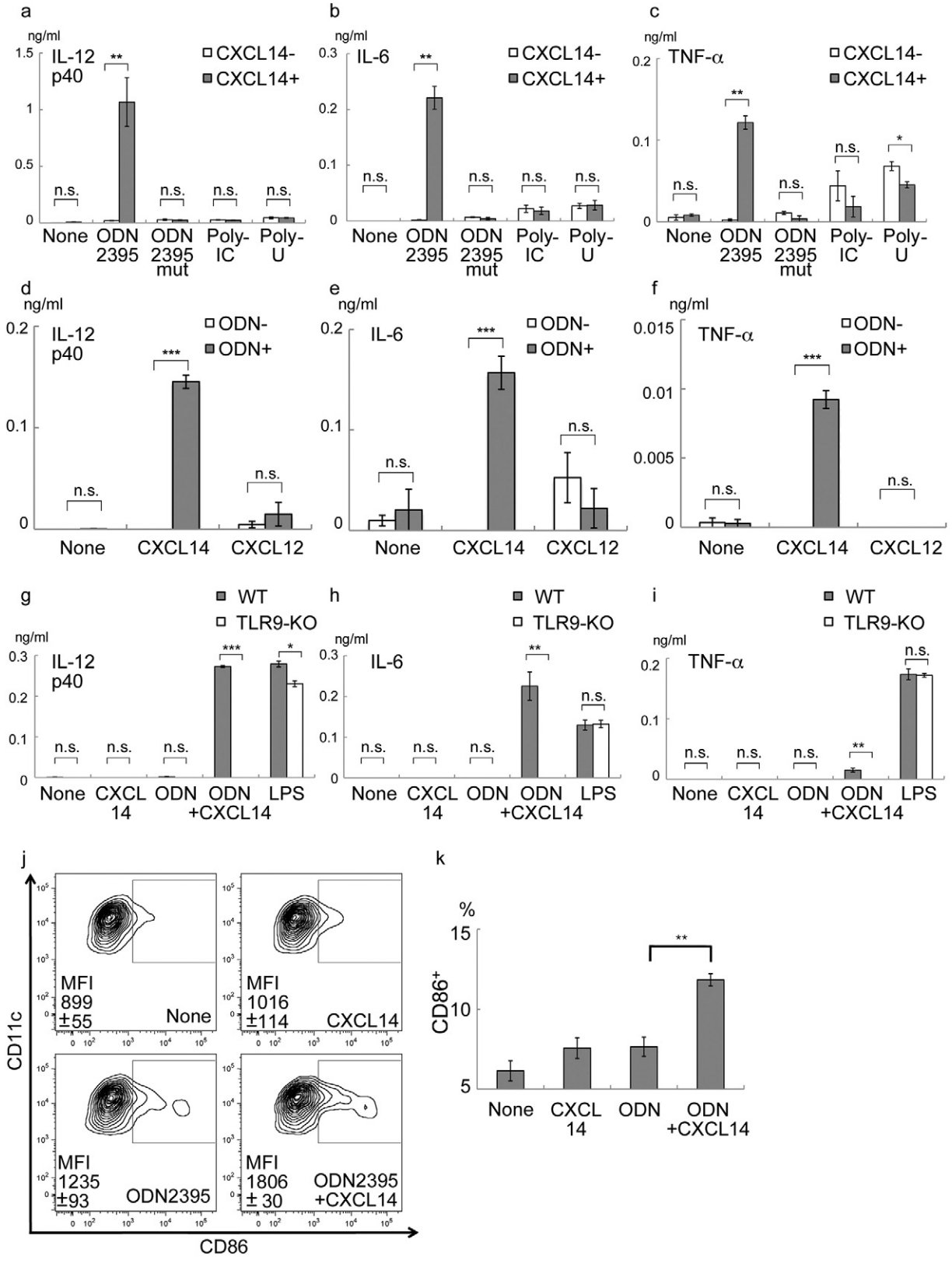

Fig. 3. Synergistic effects of CpG ODN and CXCL14 in DCs. (a–c) BMDCs were treated with 100 nM ODN2395 (ODN), 100 nM ODN2395mut (ODNmut), Poly-IC (1 μg/ml), or Poly-U (10 μg/ml) in the presence (+) or absence (−) of 300 nM CXCL14 at 37 °C for 6 h. (d–f) BMDCs were treated with 300 nM CXCL14 or CXCL12 in the presence or absence of 100 nM ODN2395 at 37 °C for 6 h. (g–i) BMDCs from WT or TLR9-KO mice were incubated with 100 nM ODN2395 in the presence or absence of 300 nM CXCL14 at 37 °C for 6 h. LPS (1 ng/ml) was used as a positive control. In a–i, conditioned media were used in an ELISA to detect IL-12 p40 (a, d, g), IL-6 (b, e, h), or TNF-α (c, f, i). (j) BMDCs were treated with 100 nM ODN2395 in the presence or absence of 300 nM CXCL14 at 37 °C for 24 h. CD86 expression by $CD11c^+$ BMDCs was examined by FACS. $CD86^+$ fractions are boxed. (k) Percentage of each $CD86^+$ population in (j). In A–I and K, each value represents the mean ± SE ($n = 3$; $^*P < 0.05$, $^{**}P < 0.01$, $^{***}P < 0.001$; n.s., not significant).

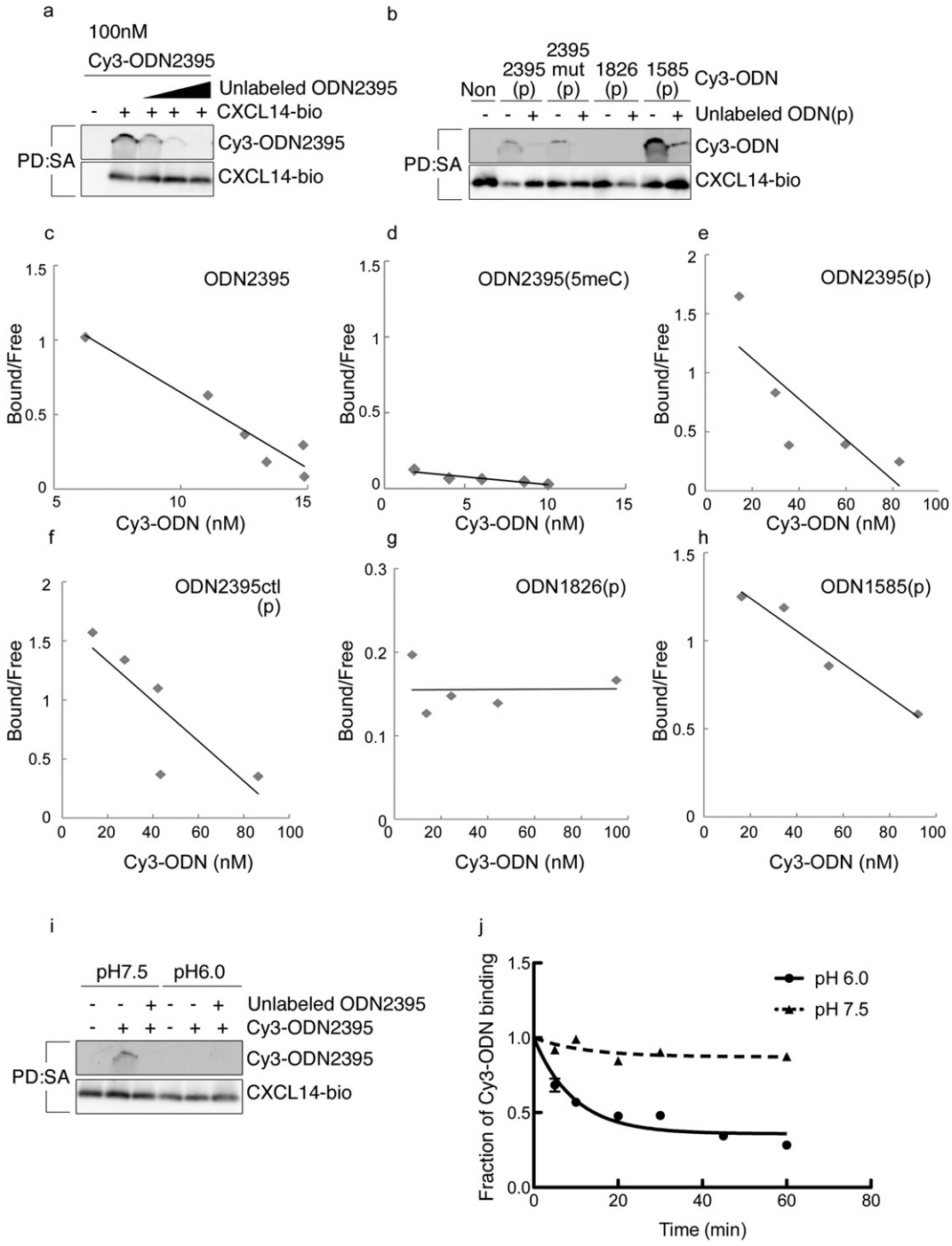

Fig. 4. Specific binding of CXCL14 to CpG ODN. (a, b) 100 nM Cy3-labeled CpG ODN was incubated with 100 nM biotinylated CXCL14 in the presence or absence of unlabeled CpG ODN (1, 10, or 100× in A; 100× in B) at 4 °C for 1 h. The complex was then pulled down with streptavidin-agarose (SA). CpG ODN and CXCL14 in the precipitate were visualized by gel electrophoresis and Western blotting with the indicated antibodies. (c–h) Scatchard plots. Different amounts of Cy3-labeled CpG ODN were subjected to a CXCL14 pulled-down assay. Bound and free Cy3 fluorescence was quantified. (i) Cy3-labeled 100 nM ODN2395 was incubated with 100 nM biotinylated CXCL14 in the presence or absence of unlabeled ODN2395 at pH 7.5 or pH 6.0. CpG ODN and CXCL14 in the precipitate were visualized by gel electrophoresis and Western blotting with the indicated antibodies. (j) Cy3-labeled 100 nM ODN2395 and 100 nM biotinylated CXCL14 were pulled down with SA. The reaction buffer was then replaced by a buffer at pH 6.0 (solid line) or pH 7.0 (broken line), and bound and free Cy3 fluorescence was measured periodically.

interacted specifically with Cy3-ODN2395(p), Cy3-ODN2395mut(p), and Cy3-ODN1585(p), but not with Cy3-ODN1826(p), in the in vitro binding assay (Fig. 4b).

We next performed Scatchard plot analyses. The data revealed that CXCL14 bound specifically to ODN2395, ODN2395(5meC), ODN2395(p), ODN2395mut(p), ODN1585(p), ODN-D-SL03, ODN21798, ODN1826, ODN1668 and D35, with K_d values of 9–100 nM (Fig. 4c–h, Fig. S8a–d, S8f, and Table 1). We did not detect a specific interaction of CXCL14 with ODN1826(p) (Fig. 4g) and an extremely weak interaction with ODN1668(p) (K_d = 1.25 μM) (Fig. S8e). ODN1585(p) was transported into DCs in a CXCL14-independent fashion (Fig. 1e and f). Importantly, methylation of cytosine residues within ODN2395 reduced its affinity for CXCL14 by nearly 10-fold (Fig. 4d), which accounts for the slight reduction in incorporation by DCs (Fig. 1g and h).

Since TLR9 is localized to acidic intracellular compartments, we examined the pH sensitivity of the complex. CXCL14 and Cy3-ODN2395

formed a stable complex at pH 7.5, but not at pH 6.0 (Fig. 4i). Cy3-ODN2395 was released from the complex as early as 7 min after switching the pH of the reaction buffer from 7.5 to 6.0 (Fig. 4j). This CpG ODN-binding property of CXCL14 is opposite to that of TLR9 (Ohto et al., 2015), ensuring efficient transfer of CpG ODN from CXCL14 to TLR9 in the endosomal/lysosomal compartment.

3.7. CXCL14 is Required for ODN2395-mediated DC Maturation and Cytokine Production

We next examined the physiological relevance of CXCL14-mediated activation of TLR9 signaling using Cxcl14-KO mice. Cxcl14$^{+/-}$ and Cxcl14$^{-/-}$ mice intravenously received 20 nmol of ODN2395, followed by measurement of both plasma IL-12 p40 concentrations and activated DC numbers. ODN2395 increased IL-12 p40 levels in Cxcl14$^{+/-}$ mice at 24 h post-administration; however, this was not the case in Cxcl14$^{-/-}$ mice (Fig. 5a). There was no difference in plasma IL-6 concentrations between Cxcl14$^{+/-}$ and Cxcl14$^{-/-}$ mice before and after ODN2395 administration (Fig. S9).

The numbers of activated MHC class II^{high} DCs in both the CD11c$^+$CD8$^+$ and CD11c$^+$CD11b$^+$ populations from CXCL14$^{-/-}$ mice after ODN2395 administration were markedly lower than those from Cxcl14$^{+/-}$ mice (Fig. 5b and c). The steady state number of DCs was similar in Cxcl14$^{+/-}$ and Cxcl14$^{-/-}$ mice. These results suggest that CXCL14 regulates CpG ODN (ODN2395)-induced DC activation in vivo.

3.8. The CXCL14/CpG ODN Complex is Transported into Cells via CXCL14 Receptors

How is the CpG ODN/CXCL14 complex transported across the plasma membrane of DCs? To answer this question, we carried out FACS-based assays to measure binding of Cy3-ODN2395 to BMDCs. Very little Cy3-ODN2395 bound to BMDCs; however, binding increased markedly upon addition of CXCL14 (K_d = 13 nM) (Fig. 6a). DEC205 is a receptor for CpG DNA in DCs (Lahoud et al., 2012). Consistent with this, we found that overexpression of *Dec205* in 293 T cells increased Cy3-ODN2395 binding (Fig. 6b). However, the Cy3-ODN2395-binding capacity of *Dec205*-transfected 293 T cells was not augmented by CXCL14 (Fig. 6b). This indicates that DCs may have distinct receptors responsible for transport of CpG ODN/CXCL14.

Although the molecular component(s) of CXCL14 receptors have not been fully elucidated, we previously reported that CXCL14 binds to CXCR4 with high affinity (Tanegashima et al., 2013). We suspected that CXCR4 might be involved in transporting the CpG ODN/CXCL14 complex; therefore, we prepared Cxcr4-deficient BMDCs from Cxcr4$^{F/F}$:LysM-Cre and Cxcr4$^{F/F}$:CD11c-Cre mice (Fig. S10) and found that cell surface binding of Cy3-ODN2395 to both Cxcr4-conditional KO (cKO) BMDCs and control Cxcr4$^{F/F}$ BMDCs was strengthened by CXCL14 (Fig. 6c). Moreover, Cxcr4$^{F/F}$:LysM-Cre BMDCs stimulated with ODN2395/CXCL14 produced IL-12 p40 in amounts comparable with those produced by $^{Cxcr4F/F}$ BMDCs (Fig. 6d). Taken together, these data suggest that CXCR4 is not a major internalization receptor for the CpG ODN/CXCL14 complex.

4. Discussion

CXCL14 is a pleiotropic chemokine with pro-inflammatory functions. However, its physiological functions and associated underlying molecular mechanisms remain to be clarified. We discovered that CXCL14 forms a stable complex with CpG ODN prior to transport into DCs, leading to a robust increase in expression of inflammatory cytokines via activation of TLR9. We also showed that DCs express specific receptors for the CpG ODN (ODN2395)/CXCL14 complex; these

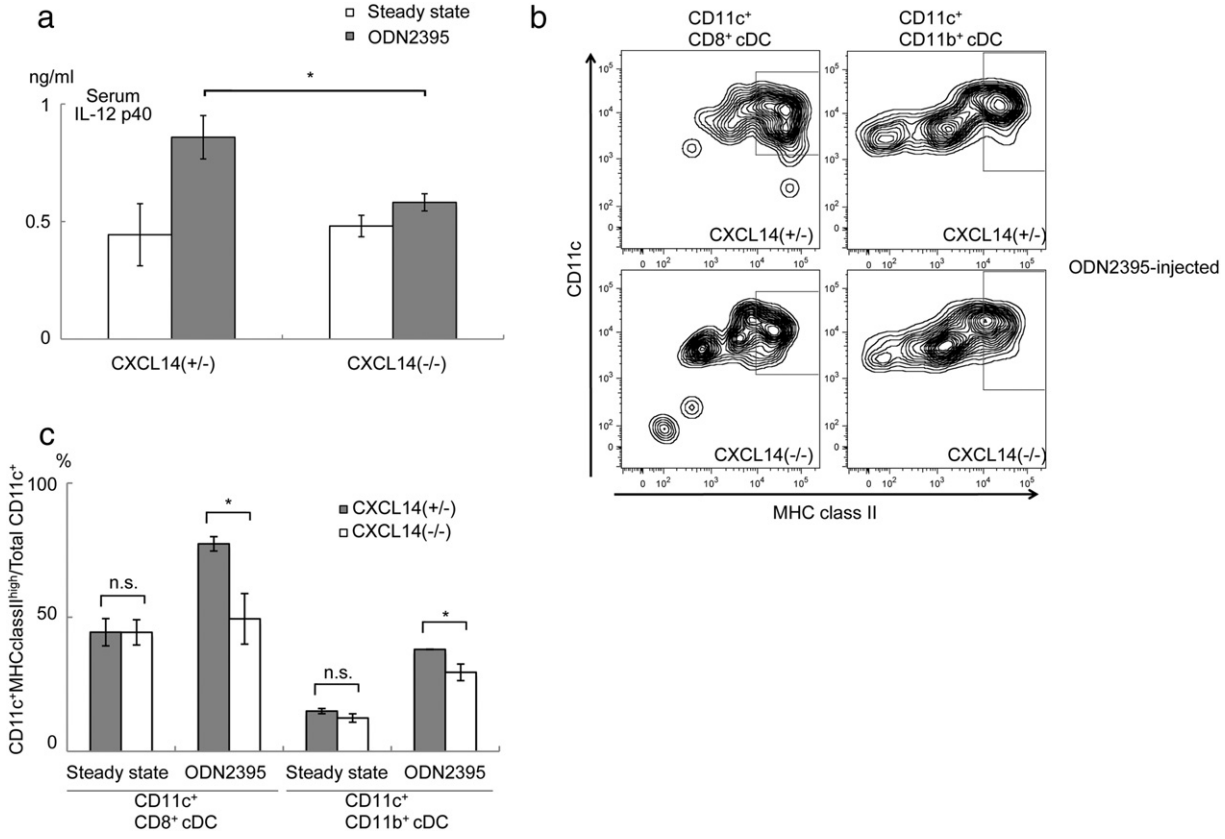

Fig. 5. In vivo responses of Cxcl14-KO mice to ODN2395. (a) Mice received an intravenous injection of ODN2395 (20 nmol) as indicated. Serum was obtained 24 h later from each mouse, and concentration of IL-12 p40 was determined by ELISA. (b) Spleens were dissected, and expression of MHC class II by CD8$^+$/CD11c$^+$ and CD11b$^+$/CD11c$^+$ DCs was determined by FACS analysis. The MHC class II^{high} fraction is boxed. (c) The percentage of MHC class II^{high} cells in (b). In A and C, each value represents the mean ± SE (n = 3; *P < 0.05; n.s., not significant).

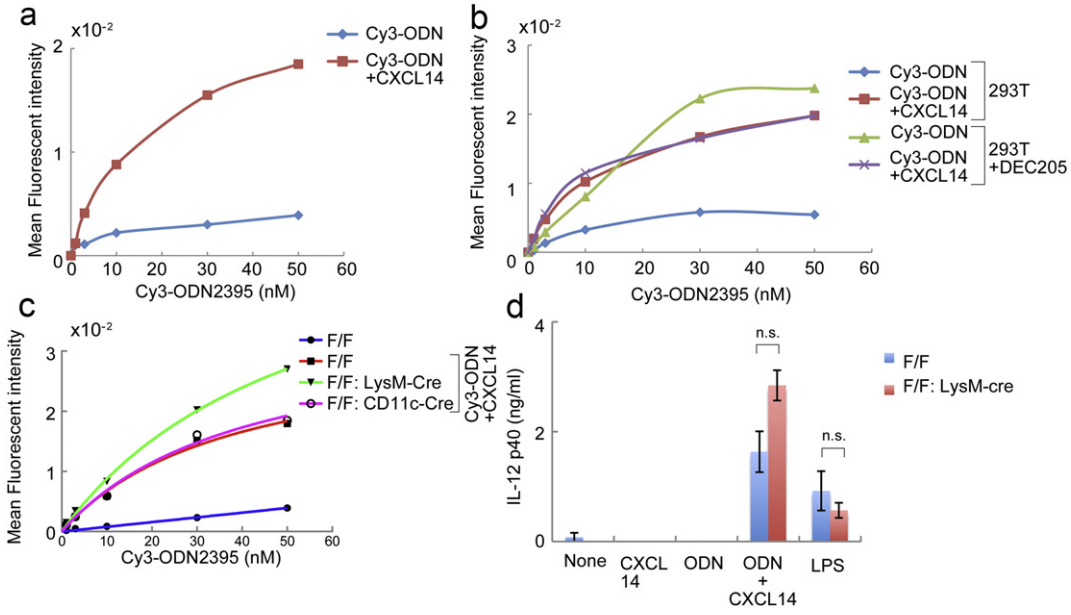

Fig. 6. Specific binding of CpG ODN/CXCL14 complex to receptors. (a) BMDCs were incubated with various concentrations of Cy3-ODN2395 in the presence or absence of 300 nM CXCL14 at 4 °C for 1 h. (b) 293 T cells or 293 T cells transfected with a DEC205 expression vector were incubated with the indicated concentrations of Cy3-ODN2395 in the presence or absence of 300 nM CXCL14. (c) BMDCs prepared from $Cxcr4^{F/F}$, $Cxcr4^{F/F}$:LysM-Cre, or $Cxcr4^{F/F}$:CD11c-Cre mice were incubated with the indicated concentrations of Cy3-ODN2395 in the presence or absence of 300 nM CXCL14. In A–C, the mean fluorescence intensity of Cy3 bound to each cell sample is shown. (d) BMDCs from $Cxcr4^{F/F}$ and $Cxcr4^{F/F}$:LysM-Cre mice were treated with 100 nM ODN2395 in the presence or absence of 300 nM CXCL14 at 37 °C for 6 h. Conditioned media ($n = 3$) were then used in an ELISA to measure IL-12 p40. LPS (1 ng/ml) was used as a positive control. n.s., not significant.

receptors are distinct from those that bind DEC205 and CXCR4. Since the CpG ODN/CXCL14 complex dissociates rapidly in the acidic endosomal/lysosomal compartments, CpG ODN is efficiently transferred to TLR9. The blunted responses of Cxcl14-KO mice to CpG ODN confirmed that CXCL14 plays a physiological role in TLR9-mediated DNA sensing. CXCL16 promotes B-class CpG ODN-mediated activation of TLR9 in DCs (Gursel et al., 2006). The present study is therefore the second to show chemokine involvement in the TLR9 system; however, here we provided the biochemical basis for the chemokine-DNA interaction.

Since TLR9 is present in the endosomal/lysosomal compartment, internalization of microbial unmethylated CpG DNA is the first event that activates the TLR9 signaling pathway (Ishii and Akira, 2006). Here, we show that CXCL14 induces internalization of CpG ODNs into DCs via high affinity binding between 1) CpG ODNs and CXCL14, and 2) the CpG ODN/CXCL14 complex and CXCL14 receptors. Previous studies identified several CpG DNA receptors and secretory factors that facilitate internalization of CpG ODNs. Granulin, HMGB1, β-defensin, and LL-37 act mainly on B-class CpG ODNs (Park et al., 2011; Ivanov et al., 2007; Hurtado and Peh, 2010; Tewary et al., 2013). Because CXCL14 interacts with various types of CpG ODNs, its spectrum is different from that of previously described CpG ODN-associated molecules.

CXCL14 and bactericidal peptides share some biochemical properties with β-defensin and LL-37 (Dai et al., 2015). CXCL14 also possesses bacteria-killing activity (Maerki et al., 2009). Indeed, clearance of *Streptococcus pneumoniae* is significantly impaired in CXCL14-KO mice (Dai et al., 2015). From the viewpoint of pathogen sensing, it is an advantage if bactericidal peptides escort CpG DNAs into DCs and activate TLR9. CXCL14 binds to CpG ODNs with a much higher affinity than β-defensin (Tewary et al., 2013). We also show that CXCL14 has reduced affinity for methylated CpG ODNs, implying that unmethylated bacterial CpG DNAs could be preferentially bound by CXCL14. Thus, CXCL14 contributes to anti-bacterial immune defenses by acting as a direct bactericidal peptide and as a carrier protein for CpG DNA.

We demonstrated that DEC205 is not involved in transport of the CpG ODN (ODN2395)/CXCL14 complex (Lahoud et al., 2012). Furthermore, Cxcr4-deficient DCs incorporated the CpG ODN/CXCL14 complex as efficiently as WT DCs. Although this does not officially rule out the possibility that CXCR4 plays a role, it suggests the existence of other CXCL14 receptor molecule(s). Identification of a responsible CXCL14 receptor molecule is necessary if we are to fully understand the mechanism underlying CpG DNA/CXCL14-mediated activation of TLR9.

TLR9 first activates the innate immune response and then triggers Th1 inflammatory responses linked to adaptive immunity (Krieg, 2006). Taking advantage of this property, CpG ODNs have been used as adjuvants for vaccines against infectious diseases and malignant cancers (Scheiermann and Klinman, 2014). Recent clinical trials of CpG ODNs show favorable outcomes (Scheiermann and Klinman, 2014). However, the efficacy of CpG ODN as a cancer vaccine adjuvant remains unsatisfactory (Scheiermann and Klinman, 2014). Here, we show that CXCL14 increases the efficiency with which CpG ODN is incorporated into both cDCs and pDCs, even in the presence of low concentrations of CpG ODN. Therefore, CXCL14 is a useful tool for delivering CpG ODNs. Clinical trials have examined high doses of CpG7909 (B-class ODN) as a cancer vaccine adjuvant (Murad et al., 2007; Scheiermann and Klinman, 2014), suggesting that administration of other ODNs in combination with CXCL14 is an attractive option for anti-cancer immunotherapy. This notion is supported by the results of a study showing NK/NKT cell-dependent suppression of the growth of B16F10 melanoma and Lewis lung carcinoma in CXCL14 transgenic mice (Hata et al., 2015). We are currently investigating the anti-tumor activity of this combined vaccine adjuvant.

Recent studies show that extracellular self-DNAs trigger obesity-induced inflammation via TLR9, resulting in insulin resistance (Revelo et al., 2016; Nishimoto et al., 2016). However, it is unclear how these DNAs are incorporated by macrophages or DCs prior to initiation of inflammatory responses. We previously showed that Cxcl14-KO mice are resistant to obesity-induced diabetes (Nara et al., 2007). Since expression of CXCL14 is upregulated in adipose tissues upon obesity, TLR9 signaling triggered by the CXCL14/self-DNA complex might contribute to insulin resistance induced by chronic inflammation. Consistent with this, a recent report shows that administration of a TLR9 inhibitory oligonucleotide (iODN) improves the insulin resistance of

obese mice (Nishimoto et al., 2016). If CXCL14 increases intracellular transport of iODN, CXCL14 might also be applicable as a therapy for obesity-induced diabetes.

We recently developed a "one-pot" synthetic procedure to generate a full length CXCL14 peptide (Tsuji et al., 2015). In terms of CpG ODN escort activity, the synthetic CXCL14 molecule is superior to *E. coli*-derived recombinant CXCL14 (unpublished data). Synthetic CXCL14 mutants will be valuable tools for elucidating structure-function relationships between CpG ODN and CXCL14. The discovery of a "minimum molecular module" that recognizes CpG would advance basic research into adaptive immunity and open new clinical applications.

Conflicts of Interest

K.T., R.T., K.T., A.S., A.O., and T.H. have a patent pending. No other authors have any competing financial interests to declare.

Author Contributions

K.T. conceived and performed most of the experiments, analyzed the data, and wrote the manuscript. R.T. and R.I. performed the DC assays. H.N. performed confocal microscopy analyses. N.N., K.T., A.S., and A.O. designed and synthesized the CXCL14 mutant peptides. T.H. designed the study, analyzed the data, and wrote the manuscript.

Acknowledgements and Funding Sources

We would like to thank Dr. Irmgard Förster for providing the LysM-Cre mice. This work was supported in part by JSPS KAKENHI grant numbers JP25860304 (K.T.), JP23390256 (T.H.), and JP16H02611 (A.O.), and by a grant from the Takeda Science Foundation (K.T.). These funding sources have no roles in design and interpretation of experiments.

Appendix A. Supplementary data

Supplementary data to this article can be found online at http://dx.doi.org/10.1016/j.ebiom.2017.09.012.

References

Blasius, A.L., Beutler, B., 2010. Intracellular toll-like receptors. Immunity 32, 305–315.
Caminschi, I., Meuter, S., Heath, W.R., 2013. DEC-205 is a cell surface receptor for CpG oligonucleotides. Oncoimmunology 2, e23128.
Chen, L., Guo, L., Tian, J., He, H., Marinova, E., Zhang, P., Zheng, B., Han, S., 2010. Overexpression of CXC chemokine ligand 14 exacerbates collagen-induced arthritis. J. Immunol. 184, 4455–4459.
Clausen, B.E., Burkhardt, C., Reith, W., Renkawitz, R., Förster, I., 1999. Conditional gene targeting in macrophages and granulocytes using LysMcre mice. Transgenic Res. 8, 265–277.
Dai, C., Basilico, P., Cremona, T.P., Collins, P., Moser, B., Benarafa, C., Wolf, M., 2015. CXCL14 displays antimicrobial activity against respiratory tract bacteria and contributes to clearance of *Streptococcus pneumoniae* pulmonary infection. J. Immunol. 194, 5980–5989.
Gursel, M., Verthelyi, D., Gursel, I., Ishii, K.J., Klinman, D.M., 2002. Differential and competitive activation of human immune cells by distinct classes of CpG oligodeoxynucleotide. J. Leukoc. Biol. 71, 813–820.
Gursel, M., Gursel, I., Mostowski, H.S., Klinman, D.M., 2006. CXCL16 influences the nature and specificity of CpG-induced immune activation. J. Immunol. 177, 1575–1580.
Hara, T., Tanegashima, K., 2012. Pleiotropic functions of the CXC-type chemokine CXCL14 in mammals. J. Biochem. 151, 469–476.
Hata, R., Izukuri, K., Kato, Y., Sasaki, S., Mukaida, N., Maehata, Y., Miyamoto, C., Akasaka, T., Yang, X., Nagashima, Y., Takeda, K., Kiyono, T., Taniguchi, M., 2015. Suppressed rate of carcinogenesis and decreases in tumour volume and lung metastasis in CXCL14/BRAK transgenic mice. Sci Rep 5, 9083.
Heit, A., Huster, K.M., Schmitz, F., Schiemann, M., Busch, D.H., Wagner, H., 2004. CpG-DNA aided cross-priming by cross-presenting B cells. J. Immunol. 172, 1501–1507.
Hemmi, H., Takeuchi, O., Kawai, T., Kaisho, T., Sato, S., Sanjo, H., Matsumoto, M., Hoshino, K., Wagner, H., Takeda, K., Akira, S., 2000. A Toll-like receptor recognizes bacterial DNA. Nature 408, 740–745.
Hurtado, P., Peh, C.A., 2010. LL-37 promotes rapid sensing of CpG oligodeoxynucleotides by B lymphocytes and plasmacytoid dendritic cells. J. Immunol. 184, 1425–1435.
Ishii, K.J., Akira, S., 2006. Innate immune recognition of, and regulation by, DNA. Trends Immunol. 27, 525–532.
Ivanov, S., Dragoi, A.M., Wang, X., Dallacosta, C., Louten, J., Musco, G., Sitia, G., Yap, G.S., Wan, Y., Biron, C.A., Bianchi, M.E., Wang, H., Chu, W.M., 2007. A novel role for HMGB1 in TLR9-mediated inflammatory responses to CpG-DNA. Blood 110, 1970–1981.
Kawai, T., Akira, S., 2010. The role of pattern-recognition receptors in innate immunity: update on toll-like receptors. Nat. Immunol. 11, 373–384.
Krieg, A.M., 2006. Therapeutic potential of toll-like receptor 9 activation. Nat. Rev. Drug Discov. 5, 471–484.
Krug, A., French, A.R., Barchet, W., Fischer, J.A., Dzionek, A., Pingel, J.T., Orihuela, M.M., Akira, S., Yokoyama, W.M., Colonna, M., 2004a. TLR9-dependent recognition of MCMV by IPC and DC generates coordinated cytokine responses that activate antiviral NK cell function. Immunity 21, 107–119.
Krug, A., Luker, G.D., Barchet, W., Leib, D.A., Akira, S., Colonna, M., 2004b. Herpes simplex virus type 1 activates murine natural interferon-producing cells through toll-like receptor 9. Blood 103, 1433–1437.
Lahoud, M.H., Ahmet, F., Zhang, J.G., Meuter, S., Policheni, A.N., Kitsoulis, S., Lee, C.N., O'Keeffe, M., Sullivan, L.C., Brooks, A.G., Berry, R., Rossjohn, J., Mintern, J.D., Vega-Ramos, J., Villadangos, J.A., Nicola, N.A., Nussenzweig, M.C., Stacey, K.J., Shortman, K., Heath, W.R., Caminschi, I., 2012. DEC-205 is a cell surface receptor for CpG oligonucleotides. Proc. Natl. Acad. Sci. U. S. A. 109, 16270–16275.
Lu, J., Chatterjee, M., Schmid, H., Beck, S., Gawaz, M., 2016. CXCL14 as an emerging immune and inflammatory modulator. J. Inflamm. 13 (1).
Lund, J., Sato, A., Akira, S., Medzhitov, R., Iwasaki, A., 2003. Toll-like receptor 9-mediated recognition of Herpes simplex virus-2 by plasmacytoid dendritic cells. J. Exp. Med. 198, 513–520.
Maerki, C., Meuter, S., Liebi, M., Muhlemann, K., Frederick, M.J., Yawalkar, N., Moser, B., Wolf, M., 2009. Potent and broad-spectrum antimicrobial activity of CXCL14 suggests an immediate role in skin infections. J. Immunol. 182, 507–514.
Moseman, A.P., Moseman, E.A., Schworer, S., Smirnova, I., Volkova, T., von Andrian, U., Poltorak, A., 2013. Mannose receptor 1 mediates cellular uptake and endosomal delivery of CpG-motif containing oligodeoxynucleotides. J. Immunol. 191, 5615–5624.
Murad, Y.M., Clay, T.M., Lyerly, H.K., Morse, M.A., 2007. CPG-7909 (PF-3512676, ProMune): toll-like receptor-9 agonist in cancer therapy. Expert. Opin. Biol. Ther. 7, 1257–1266.
Nara, N., Nakayama, Y., Okamoto, S., Tamura, H., Kiyono, M., Muraoka, M., Tanaka, K., Taya, C., Shitara, H., Ishii, R., Yonekawa, H., Minokoshi, Y., Hara, T., 2007. Disruption of CXC motif chemokine ligand-14 in mice ameliorates obesity-induced insulin resistance. J. Biol. Chem. 282, 30794–30803.
Nishimoto, S., Fukuda, D., Higashikuni, Y., Tanaka, K., Hirata, Y., Murata, C., Kim-Kaneyama, J.R., Sato, F., Bando, M., Yagi, S., Soeki, T., Hayashi, T., Imoto, I., Sakaue, H., Shimabukuro, M., Sata, M., 2016. Obesity-induced DNA released from adipocytes stimulates chronic adipose tissue inflammation and insulin resistance. Sci. Adv. 2, e1501332.
Ohto, U., Shibata, T., Tanji, H., Ishida, H., Krayukhina, E., Uchiyama, S., Miyake, K., Shimizu, T., 2015. Structural basis of CpG and inhibitory DNA recognition by Toll-like receptor 9. Nature 520, 702–705.
Park, B., Buti, L., Lee, S., Matsuwaki, T., Spooner, E., Brinkmann, M.M., Nishihara, M., Ploegh, H.L., 2011. Granulin is a soluble cofactor for toll-like receptor 9 signaling. Immunity 34, 505–513.
Revelo, X.S., Ghazarian, M., Chng, M.H., Luck, H., Kim, J.H., Zeng, K., Shi, S.Y., Tsai, S., Lei, H., Kenkel, J., Liu, C.L., Tangsombatvisit, S., Tsui, H., Sima, C., Xiao, C., Shen, L., Li, X., Jin, T., Lewis, G.F., Woo, M., Utz, P.J., Glogauer, M., Engleman, E., Winer, S., Winner, D.A., 2016. Nucleic acid-targeting pathways promote inflammation in obesity-related insulin resistance. Cell Rep. 16, 717–730.
Roda, J.M., Parihar, R., Carson 3rd., W.E., 2005. CpG-containing oligodeoxynucleotides act through TLR9 to enhance the NK cell cytokine response to antibody-coated tumor cells. J. Immunol. 175, 1619–1627.
Samulowitz, U., Weber, M., Weeratna, R., Uhlmann, E., Noll, B., Krieg, A.M., Vollmer, J., 2010. A novel class of immune-stimulatory CpG oligodeoxynucleotides unifies high potency in type I interferon induction with preferred structural properties. Oligonucleotides 20, 93–101.
Scheiermann, J., Klinman, D.M., 2014. Clinical evaluation of CpG oligonucleotides as adjuvants for vaccines targeting infectious diseases and cancer. Vaccine 32, 6377–6389.
Tabeta, K., Georgel, P., Janssen, E., Du, X., Hoebe, K., Crozat, K., Mudd, S., Shamel, L., Sovath, S., Goode, J., Alexopoulou, L., Flavell, R.A., Beutler, B., 2004. Toll-like receptors 9 and 3 as essential components of innate immune defense against mouse cytomegalovirus infection. Proc. Natl. Acad. Sci. U. S. A. 101, 3516–3521.
Tanegashima, K., Okamoto, S., Nakayama, Y., Taya, C., Shitara, H., Ishii, R., Yonekawa, H., Minokoshi, Y., Hara, T., 2010. CXCL14 deficiency in mice attenuates obesity and inhibits feeding behavior in a novel environment. PLoS One 5, e10321.
Tanegashima, K., Suzuki, K., Nakayama, Y., Tsuji, K., Shigenaga, A., Otaka, A., Hara, T., 2013. CXCL14 is a natural inhibitor of the CXCL12-CXCR4 signaling axis. FEBS lett. 587, 1731–1735.
Tewary, P., de la Rosa, G., Sharma, N., Rodriguez, L.G., Tarasov, S.G., Howard, O.M., Shirota, H., Steinhagen, F., Klinman, D.M., Yang, D., Oppenheim, J.J., 2013. beta-Defensin 2 and 3 promote the uptake of self or CpG DNA, enhance IFN-alpha production by human plasmacytoid dendritic cells, and promote inflammation. J. Immunol. 191, 865–874.
Tsuji, K., Tanegashima, K., Sato, K., Sakamoto, K., Shigenaga, A., Inokuma, T., Hara, T., Otaka, A., 2015. Efficient one-pot synthesis of CXCL14 and its derivative using an *N*-sulfanylethylanilide peptide as a peptide thioester equivalent and their biological evaluation. Bioorg. Med. Chem. 23, 5909–5914.
Yang, L., Wu, X., Wan, M., Yu, Y., Yu, Y., Wang, L., 2013. CpG oligodeoxynucleotides with double stem-loops show strong immunostimulatory activity. Int. Immunopharmacol. 15, 89–96.